

Improving the Description of the Optical Properties of Carotenoids by Tuning the Long-Range Corrected Functionals

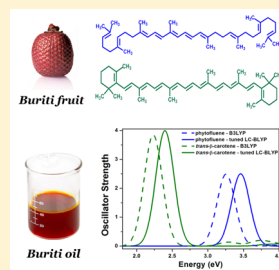
Igo T. Lima,^{†,¶} Andriele da S. Prado,[†] João B. L. Martins,[‡] Pedro Henrique de Oliveira Neto,[†] Artemis M. Ceschin,[§] Wiliam F. da Cunha,[†] and Demétrio A. da Silva Filho^{*,†}

[†]Institute of Physics, [‡]Institute of Chemistry, and [§]Electrical Engineering Department, University of Brasília, 70919-970 Brasília, Brazil

[¶]Federal University of Maranhão, 65800-000 Balsas, Maranhão Brazil

Supporting Information

ABSTRACT: In this work we use *gap-fitting* procedure to tune the long-range corrected functionals and accurately investigate the electronic and optical properties of the five main molecules composing Buriti oil (extracted from *Mauritia flexuosa* L.) in the framework of density functional theory (DFT) and time-dependent (TD) DFT. The characteristic length ($1/\omega$) was observed to be entirely system dependent, though we concluded that its determination is of fundamental importance to rescue geometrical, electronic, and optical properties with accuracy. We demonstrate that our approach of tuning characteristic length for each system resulted in an absorbance spectra in better experimental agreement when compared to the traditional methodology. Therefore, this study indicates that the tuning of the range-separation parameter is crucial to improve the description of the optical properties of conjugated molecules when TDDFT is used. For example, the wavelength of maximum absorption, λ_{max} for the phytofluene, obtained using B3LYP, is 381 nm, while using the gap-fitting procedure for the tuned-LC-BLYP the estimated λ_{max} changed to 358 nm. The latter estimate is in better agreement with the experimental value of 350 nm.



INTRODUCTION

Among all natural pigments, carotenoids, a group of over 700 compounds—500 of which have established electronic structures¹—are probably the most abundantly found in Nature. These substances can be found in plants, animals, and microorganisms. It is suggested that they present antioxidant properties and act as an efficient inhibitor of cell proliferation, allowing its use as a preventive factor to human prostate cancer,² for example.

Formed by 40 carbon atoms, the feature that stands out the most in the structure of these molecules is the presence of long chains of conjugated double bonds. This is responsible for many of their physical–chemical properties and biological functions. This kind of conjugation pattern is known to yield interesting optical and electronic properties for organic systems in general³ and suggests a potential use of carotenoids to the development of organic photovoltaics.⁴ Because of their interesting electronic and optical properties, they have been already used in dye-sensitized solar cells.⁵

A widely available source of carotenoids found in Brazilian flora is a kind of palm tree called Buriti (*Mauritia flexuosa* L.). Growing near wet areas in South America, the oil extracted from the Buriti fruit is extremely rich in carotenoids of several kinds. It has been found that the Buriti oil absorbs strongly in the visible region; ultraviolet radiation absorption is also reported. Studies by Durães and co-workers⁶ stress the fact that Buriti oil has interesting optical properties such as photoluminescence. This points toward the possibility of using Buriti oil to improve the absorption and emission of light from polymer matrices polystyrene (PS) and poly(methyl meth-

acrylate) (PMMA).^{7,8} Buriti oil is used mainly as a natural sunscreen, but its absorption and emission properties make it a promising “green” material in the design of electronic devices based on organic molecules.

In this context, we investigate the electronic and optical properties of the main carotenoid molecules present in the Buriti oil. The π -conjugated backbone combined with terminal isoprenoid rings present in these substances has been extensively studied by theoretical methods^{9,10} and optical spectroscopy.¹¹ They absorb strongly in the visible region between 400 and 500 nm (trans isomers), while cis and cis/trans isomers also exhibit an absorption band near-ultraviolet (UV) region, around 320 nm. Also, the bond conjugation present in the backbone of carotenoids shows that these molecules are true representatives of the conjugated polymer class, which means that their charge carriers can show high mobility depending on external conditions and excitations.¹² An interesting approach to model this type of many body system is by means of density functional theory (DFT).

Indeed, DFT method combined with B3LYP^{13–15} hybrid functional has been widely used to study the electronic structure and optical properties of molecules such as carotenoids. However, it is well-known that the traditional

Special Issue: Piergiorgio Casavecchia and Antonio Lagana Festschrift

Received: December 23, 2015

Revised: February 17, 2016

Published: February 17, 2016



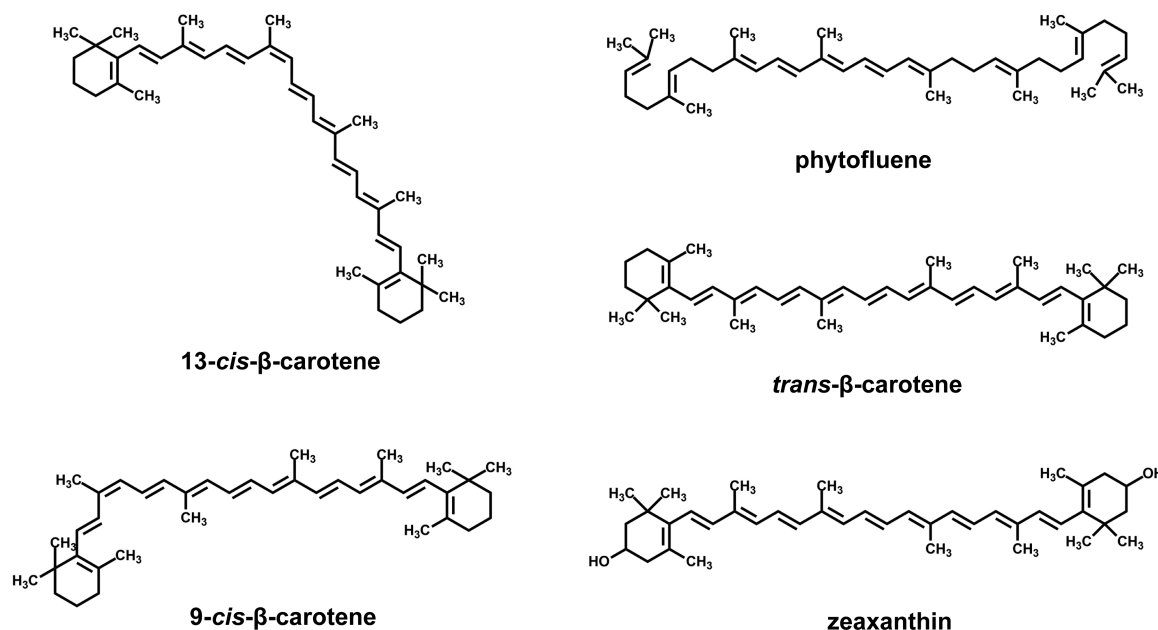


Figure 1. Carotenoid molecules investigated in this work.

DFT functionals tends to promote a delocalization of the system's wave function.¹⁶ This fact is a major challenge when modeling organic semiconductors, as it is known that localized quasiparticles are responsible for the charge transport in these systems. The recently developed long-range corrected (LRC)^{17,18} functionals with tuning range separation parameter^{19,20} has been successfully used to overcome this kind of difficulty. The central idea in the design of these LRC functionals is the partitioning of the Coulomb operator into short-range (SR) and long-range (LR) components with the help of the standard error function (erf):

$$\frac{1}{r} = \frac{\text{erf}(\omega r)}{r} + \frac{\text{erfc}(\omega r)}{r} \quad (1)$$

In this expression, the first term represents a semilocal functional approximation that describes the SR, and second term represents the full inclusion of exact exchange in the LR. In this way, LR corrected functionals should, in principle, improve the description of excited states with a charge-transfer character.

Martins et al.⁷ have conducted a study on the spectra of these carotenoid molecules in the scope of several methods, including DFT, which, incidentally yielded the best results. Coccia et al. has highlighted the challenge to accurately determine the ground-state geometry of carotenoids due to the poor description of electronic correlation present in conjugated polyenic chains.¹⁰

In the present work, we propose the use of LRC to obtain electronic and optical properties of these carotenoid molecules in a more precise and molecule-customized fashion. Time-dependent DFT (TDDFT) calculations with functional that includes LR corrections considering globally tuned ω parameter dedicated to each system are also performed. We show how this procedure is observed to be superior to the standard DFT method as far as static and optical properties are concerned.

This work is organized as follows: in the next section we describe the **Computation Details** together with a brief explanation of the ω tuning procedure. Following, our results are presented together with their discussion. We finish the

paper reporting the main conclusions and contributions of this work.

■ COMPUTATIONAL DETAILS

The chemical structures of five carotenoid molecules examined in this work are presented in **Figure 1**. As a common trait, we can see that all molecules have isoprene groups—that could act as an electron acceptor in an organic electronic device—and a backbone bridge—a possible donor. We noted that four of the five carotenoid systems have the conjugated backbone with nine double bonds. Phytofluene, however, presents the conjugation pathway with five double bonds. Because of the shorter conjugation length, it is expected, a priori, a different behavior of electronic and optical properties for phytofluene when compared to the other systems, as will be further discussed.

Optical excitations in these polymers can be computed within the TDDFT formalism. Nevertheless, the use of conventional semilocal and standard hybrid DFT functionals (such as the popular B3LYP functional) can lead to poor descriptions of charge-transfer like excitations²¹ due to limitations associated with the lack of LR exchange interactions.²² Among the strategies to overcome these limitations, LRC functionals represent a relatively new class of functionals for generalized Kohn–Sham theory that has proven to be very successful, for instance, when it comes to predicting ionization potentials²³ and energy gaps for a wide range of molecules. In this work we employ LRC functionals, where the range-separation parameter (ω) is tuned through a gap-fitting procedure presented by Baer and Kronik:^{24–26}

$$J_{\text{IP}}(\omega) = |\epsilon_{\text{H}}^{\omega}(N) + E_{\text{gs}}^{\omega}(N-1) - E_{\text{gs}}^{\omega}(N)| \quad (2)$$

$$J_{\text{EA}}(\omega) = |\epsilon_{\text{H}}^{\omega}(N+1) + E_{\text{gs}}^{\omega}(N) - E_{\text{gs}}^{\omega}(N+1)| \quad (3)$$

$$J_{\text{gap}}(\omega) = \sqrt{(J_{\text{IP}}(\omega))^2 + (J_{\text{EA}}(\omega))^2} \quad (4)$$

where $\epsilon_{\text{H}}^{\omega}(N)$ is the highest occupied molecular orbital (HOMO) energy for an N -electron system, and $E_{\text{gs}}^{\omega}(N)$ is the

corresponding self-consistent field (SCF) energy. Analogously, $\epsilon_H^\omega(N+1)$ is the singly occupied molecular orbital (SOMO) energy for an $N+1$ electron system, and $E_{gs}^\omega(N+1)$ and $E_{gs}^\omega(N-1)$ are the corresponding SCF energies of the anion and cation states, respectively.

The ω tuning through eqs 2–4 can lead to an improvement in the description of the properties calculated using LRC functionals. This approach has been recently employed to study the optical properties of DA copolymers with great success.^{20,27} Starting with the optimized B3LYP/6-31G(d,p)^{28,29} structure, the range-separation parameter (ω) and the systems geometry are iteratively tuned to ensure that the HOMO–LUMO (LUMO = lowest unoccupied molecular orbital) gap, obtained from the tuned functional, can be directly comparable to the quasi-particle gap. The basis set was selected due to its good track record with similar organic systems.^{7,30} Exploratory calculations show that the addition of diffuse functions does little changes in the properties under investigation.

Low-lying singlet excited states were evaluated at the TD-DFT level with iteratively tuned LC-BLYP^{18,22} and ω B97³¹ optimized geometries using the 6-31G(d,p) basis set. Optical absorption profiles were simulated through convolution of the stick transitions (characterized by a given wavelength and oscillator strength) with Gaussian functions with a full width at half-maximum (fwhm) of 0.3 eV. All calculations were performed with Gaussian 09 (Rev.D.01)³² software suite.

RESULTS AND DISCUSSION

ω Optimization. We start our discussion presenting the results for the ω optimization. Table 1 shows the tuned values

Table 1. Tuned ω^a (bohr⁻¹) and Characteristic Length $1/\omega$ (bohr) for the Five Carotenoids Determined at LC-BLYP and ω B97 Level Using the Same 6-31G(d,p) Basis Set

| molecule | tuned LC-BLYP | | tuned ω B97 | |
|------------------------------------|---------------|------------|--------------------|------------|
| | ω | $1/\omega$ | ω | $1/\omega$ |
| 13- <i>cis</i> - β -carotene | 0.152 | 6.579 | 0.150 | 6.667 |
| 9- <i>cis</i> - β -carotene | 0.152 | 6.579 | 0.150 | 6.667 |
| phytofluene | 0.193 | 5.181 | 0.187 | 5.347 |
| <i>trans</i> - β -carotene | 0.151 | 6.622 | 0.149 | 6.711 |
| zeaxanthin | 0.149 | 6.711 | 0.147 | 6.803 |

^aThe default values for the (ω) are $\omega_{(\text{LCBLYP})} = 0.47$ and $\omega_{(\omega \text{B97})} = 0.4$ Bohr⁻¹ as implemented in G09.³²

of the range-separation parameter (ω) and the corresponding characteristic length values ($1/\omega$) of the carotenoids obtained with LC-BLYP and ω B97 functionals and using the 6-31G(d,p) basis set. With exception of the phytofluene, all molecules showed ω and $1/\omega$ values that are quite similar and have little dependence on the used functional. This is a consequence of the different structure of the phytofluene compared to the other systems that present the totally conjugated backbone. As we will present later, the differences in geometry and in the tuned ω values are reflected in the electronic and optical properties of these molecules. It is also worth mentioning that the ω value that minimizes the J_{gap} is essentially the same as the one that minimizes J_{IP} (see Figure S1 in Supporting Information).

Geometric Properties. We now turn to the characterization of the geometrical properties and the impact of the ω optimization on it. We noted that—with the exception of phytofluene—all five molecules present nine double bonds on the main chain. The lower degree of conjugation of

phytofluene, that is, five double bonds on the main chain, should affect significantly the characteristic length ($1/\omega$) as well as in the electronic and optical properties. We begin our discussion looking at the optimized molecular geometries at the ground state. Figure 2 and Table 2 provide definitions and collect representative torsion angles along the main chain of the five molecules.

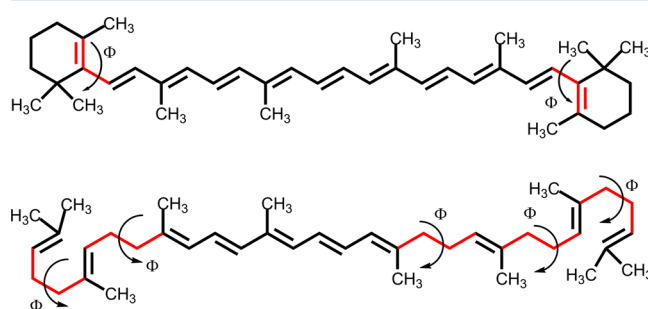


Figure 2. Torsion angles along the main chain of the carotenoids.

Table 2. Torsion Angles Values (Φ) along the Main Chain of the Carotenoids

| molecule | B3LYP | tuned-LC-BLYP | tuned- ω B97 |
|------------------------------------|-------|---------------|---------------------|
| 13- <i>cis</i> - β -carotene | 48° | 42° | 51° |
| 9- <i>cis</i> - β -carotene | 48° | 41° | 51° |
| phytofluene | 178° | 178°, 179° | 178°, 179° |
| <i>trans</i> - β -carotene | 48° | 42° | 51° |
| zeaxanthin | 47° | 41° | 51° |

We note that four of the five molecules, that is, 13-*cis*- β -carotene, 9-*cis*- β -carotene, *trans*- β -carotene, and zeaxanthin present a quite planar backbone with torsion angles at the ends due to the functional groups. In general, torsion angles values are the same when we use the same functional in the DFT calculations. The exception is the phytofluene where the optimized ground-state geometry presents significant differences at the torsion angles on the backbone due to σ -bonds at the main chain. This structural difference of the phytofluene should be manifested in the lower delocalization of the wave function at this molecule in comparison to other carotenoids.

The planarity deviations induce changes in the electronic properties of the carotenoids by reduction of the wave function delocalization. According with Körzdörfer^{19,20} the characteristic length provides an alternative way to describe the extent of the conjugation in the system. Hence, the range-separation parameter was iteratively tuned, and ground-state structures were optimized according *gap-fitting* procedure to make HOMO–LUMO gap equal to the fundamental gap of studied system when a suitable fraction of Hartree–Fock (HF) exchange is treated explicitly.³³

It is important to highlight the polyenic character of the carotenoids and the difficulties to describe the geometry of these systems by means of quantum chemical calculations.³⁴ It can be understood by looking at the bond-length alternation (BLA) behavior of these systems. BLA behavior of these systems has been a very discussed topic in the scientific community for several years, and it plays an important role in the electronic and optical properties of the conjugated molecular chains.³⁵ Jacquemin et al. demonstrated that CAM-B3LYP provides an improved description of BLA in short oligomers of *trans*-polyacetylene (PA),³⁶ while standard hybrid

DFT underestimate this parameter.^{36,37} However, it is not a simple task to obtain reliable BLA values by electronic structure methods.

In general, the Hartree–Fock theory significantly overestimates the BLA value, while MP2 and DFT, with the commonly used approximations to the exchange–correlation functional, tend to underestimate this parameter. Here, we are interested how BLA depends on the DFT functional used in the calculation. Figure 3 shows the considered chemical bonds

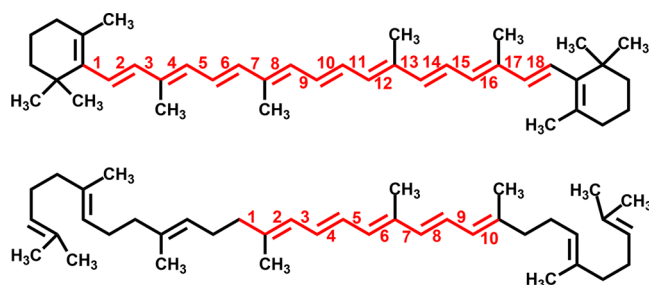


Figure 3. Chemical bonds considered in the BLA calculation along the carotenoid chains.

Table 3. BLA Values Obtained at B3LYP and LRC Functionals LC-BLYP and ω B97 using Default and Tuned ω Values

| molecule | B3LYP | LC-BLYP | ω B97 | tuned LC-BLYP | tuned ω B97 |
|------------------------------------|-------|---------|--------------|---------------|--------------------|
| 13- <i>cis</i> - β -carotene | 0.079 | 0.120 | 0.118 | 0.083 | 0.089 |
| 9- <i>cis</i> - β -carotene | 0.079 | 0.120 | 0.118 | 0.083 | 0.089 |
| phytofluene | 0.098 | 0.127 | 0.126 | 0.104 | 0.108 |
| <i>trans</i> - β -carotene | 0.078 | 0.120 | 0.118 | 0.083 | 0.089 |
| zeaxanthin | 0.076 | 0.119 | 0.117 | 0.081 | 0.087 |

used in the BLA calculation, and Table 3 shows the obtained values using different functionals. We observe that for all investigated molecules the B3LYP functional presents the smallest BLA values, while the LRC functional, with default ω values, presents the largest. This fact is associated with the amount of HF contribution to the exchange–correlation term, that is, a smaller HF contribution implies a larger delocalization for the B3LYP functional, while a larger HF contribution implies a larger wave function localization for the LRC functional.

The ω tuning procedure on the LRC functionals implies to fit this parameter and consequently decreasing of electronic (de)localization. Thus, BLA values obtained via LRC functionals with tuned ω show intermediate values, that is, lower than default-LRC and higher than B3LYP functional.

However, the ω tuning does not guarantee accurate values of BLA. Körzdörfer and co-workers³⁴ have shown similar behavior for long polyene chains, and though the *gap-fitting* procedure decrease self-interaction errors, it does not provide accurate BLA values. Therefore, it is expected that the all-conjugated carotenoids, that is, molecules with the larger conjugation length on the backbone (13-*cis*- β -carotene, 9-*cis*- β -carotene, *trans*- β -carotene, and zeaxanthin), do not show BLA values close to experimental data. This deficiency of the electronic structure theory impacts several other properties. For instance,

we will show later that an incorrect description of BLA is directly related to the position of the absorption threshold.

Electronic Properties. We now turn our attention to the description of the electronic properties of the carotenoids. As noted before, the structural difference of the phytofluene as well as structural similarities among the other molecules are manifested in the molecular orbital (MO) energies. Figure 4

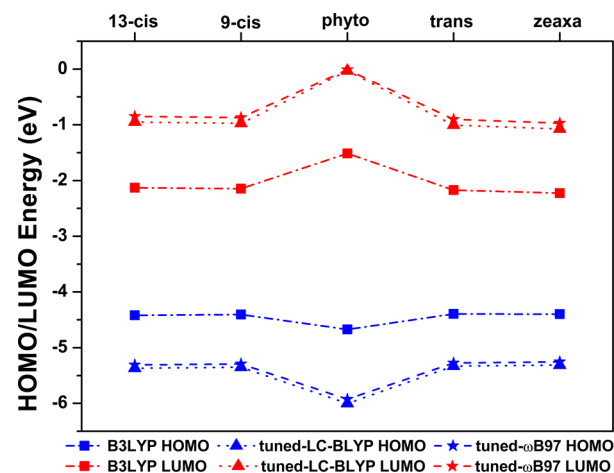


Figure 4. HOMO–LUMO values calculated for B3LYP as well as tuned LC-BLYP and ω B97 ground state of the five carotenoids.

shows frontier MO energies of the HOMO and LUMO for all carotenoids in the series, calculated using B3LYP functional as well as with the LRC functionals LC-BLYP and ω B97 (using the tuned ω values). Clearly, HOMO and LUMO energies for the phytofluene have different behaviors compared to those of other carotenoids in the series, presenting a wider HOMO–LUMO gap compared to those of the other molecules. This behavior is strictly related to the lower degree of conjugation of the phytofluene molecule. It is worth mentioning that the energy gap values obtained via LRC functionals (LC-BLYP and ω B97) are higher than for the B3LYP. It is a consequence of gap-fitting procedure on the LRC functionals. As previously clarified, the idea of the gap-fitting procedure is to obtain more realistic and localized wave functions that are important to the charge transfer processes. Hence, it is expected that the use of the gap-fitting procedure on the LRC functionals provides wider HOMO–LUMO gap compared to the B3LYP ones.

The LRC functionals, with the tuned ω parameter, provide a more localized description of the wave function of the DA copolymers. Thus, this methodology shows a better description of the electronic and optical properties of these systems. The remarkable difference among the calculated energy gap values via B3LYP and the tuned LRC functionals indicate that gap-fitting procedure is more appropriate to the description of charge transfer processes.

Figure 5 and Figures S2 and S3 (Supporting Information) illustrate the HOMO and LUMO wave function of the carotenoids calculated at LC-BLYP and ω B97 level using the 6-31G(d,p) basis set. Here we can note that for 13-*cis*- β -carotene, 9-*cis*- β -carotene, *trans*- β -carotene, and zeaxanthin, HOMO and LUMO wave functions are broadly delocalized along the conjugated backbone. This is because these molecules present planar molecular geometries and the totally conjugated main chain. The phytofluene, however, has lower degree of conjugation, and the twisted molecular geometry induces a

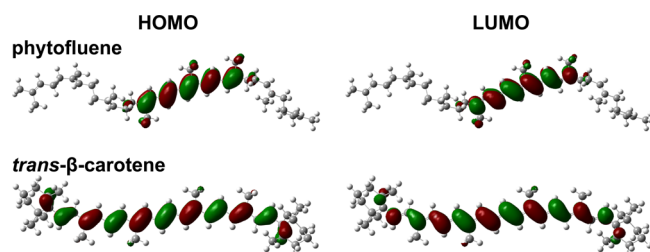


Figure 5. Molecular orbitals for phytofluene and *trans*- β -carotene: HOMO (left) and LUMO (right).

localization of the HOMO and LUMO wave function over the conjugation pathway constituted by five double bonds on the main chain.

Optical Properties. So far we detailed how lower degree of conjugation at the phytofluene structure is related to different electronic properties for this system when compared to the all-conjugated carotenoids, that is, 13-*cis*- β -carotene, 9-*cis*- β -carotene, *trans*- β -carotene, and zeaxanthin. This fact should also have an impact on the absorption spectra of the carotenoids. We performed TDDFT calculations to investigate the optical properties of these carotenoids using B3LYP and LRC functionals (LC-BLYP and ω B97 with default and tuned ω values) and the same 6-31G(d,p) basis set. Optical absorption spectra were simulated using a 0.3 eV fwhm Gaussian broadening on the vertical transition energies and associated oscillator strengths. For comparison purposes Figure 6 and Figure S4 (Supporting Information) show absorption spectra of five carotenoids computed using TD-B3LYP/6-31G(d,p), TD-LC-BLYP/6-31G(d,p), and TD- ω B97/6-31G(d,p). The most important feature here is the displacement of absorption spectra of the tuned TD-LRC functionals when compared to the traditional TD-B3LYP; that is, the maximum absorption peak is displaced to a higher energy region. Note that for phytofluene, which has the lowest conjugation pathway, the maximum absorption peak is displaced even further when compared to the values of the all-conjugated carotenoids.

Furthermore, we also performed TD-LC-BLYP/6-31G(d,p) and TD- ω B97/6-31G(d,p) with default ω values to comparison with gap-fitting method. Table 4 shows that, for phytofluene, the findings obtained via tuned LC-BLYP and ω B97 are in better agreement with experimental compared to B3LYP and default LC-BLYP and ω B97. In this case, gap-fitting procedure improved the accuracy of LRC functionals compared to the description obtained when using B3LYP and default LRC functionals. However, a smaller improvement was observed in the case of the all-conjugated molecules. This fact can be attributed to a poor description of BLA, which impacts the λ_{\max} position. For the all-conjugated molecules, the tuned LRC functionals still provide results in better agreement with experimental data when compared to B3LYP and default LRC functionals.

As mentioned previously, the electronic structure theory fails to provide a good description of the BLA parameter of long-conjugated chains and, consequently, also fails to describe the optical properties of these systems accurately.³⁴ Here we verified that DFT methods describe substantially better the phytofluene, which has lower conjugation pathway (five double bonds) than all-conjugated molecules, that is, nine double bonds on the main chain. It is worth mentioning that there are differences in the description of the λ_{\max} position among default and tuned LRC functionals, while default-LRC functionals

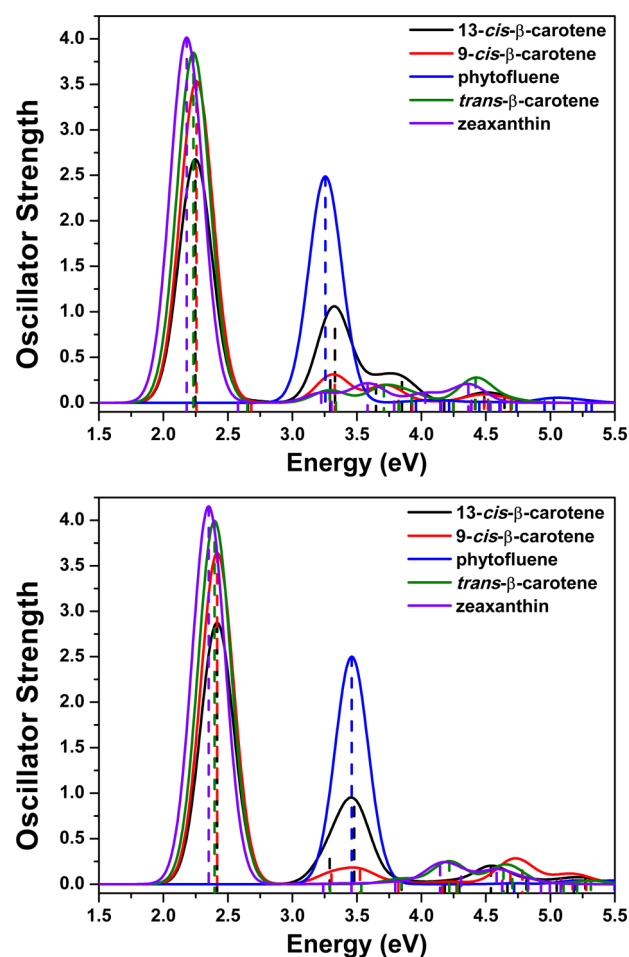


Figure 6. Absorption spectra for the five molecules computed at B3LYP (top) and tuned-LCBLYP (bottom).

Table 4. Wavelength^a of Maximum Absorbance (λ_{\max})

| molecule | 13- <i>cis</i> - β | 9- <i>cis</i> - β | phytofluene | <i>trans</i> - β | zeaxanthin |
|--------------------|--------------------------|-------------------------|-------------------|--------------------------------------|-------------------|
| experimental | 443 ³⁹ | 445 ³⁹ | 350 ³⁸ | 448, ⁴⁰ 450 ⁴¹ | 450 ⁴² |
| B3LYP | 551 | 549 | 381 | 555 | 569 |
| LC-BLYP | 348 | 350 | 293 | 352 | 355 |
| tuned LC-BLYP | 513 | 513 | 358 | 517 | 527 |
| ω B97 | 363 | 364 | 303 | 366 | 370 |
| tuned ω B97 | 507 | 506 | 362 | 511 | 522 |

^aIn nanometers. Experimental data and B3LYP and LRC functionals (LCBLYP and ω B97) with default and tuned ω values.

show displaced λ_{\max} to lower wavelength than experimental data, the tuned-LRC functionals present displaced λ_{\max} to higher wavelength. It has been attributed to the higher HF contribution on the default-LRC than tuned-LRC functionals, and consequently, default LRC functional provides a higher wave function localization compared to the same tuned-LRC functional. Table 5 and Table S1 (Supporting Information) show the vertical transition energies ($S_0 \rightarrow S_1$), oscillator strength (f), transition dipole moment (μ_{01}), and electronic configurations to analyze the nature of the $S_0 \rightarrow S_1$ absorption. The results show that the transition dipole moment is aligned predominantly to the molecular axis. Furthermore, in all cases, the vertical transition from the ground to first excited state ($S_0 \rightarrow S_1$) is predominantly from HOMO to LUMO (HOMO \rightarrow

Table 5. $S_0 \rightarrow S_1$ Vertical Transition Energies^a (E_{01}), Oscillator Strengths^a (f), Transition Dipole Moments^a (μ_{01}), and Electronic Configurations^a of Carotenoids

| molecule | E_{01} (eV) | f | μ_{01} (debye) | | | | electronic configuration (%) |
|------------------------------------|---------------|------|--------------------|-------|-------|-------|------------------------------|
| | | | x | y | z | total | |
| 13- <i>cis</i> - β -carotene | 2.41 | 2.87 | 17.69 | −0.41 | 0.02 | 17.70 | HOMO \rightarrow LUMO(94) |
| 9- <i>cis</i> - β -carotene | 2.42 | 3.64 | 19.88 | 1.25 | −0.01 | 19.92 | HOMO \rightarrow LUMO(94) |
| phytofluene | 3.46 | 2.50 | 13.17 | 4.09 | 0.07 | 13.79 | HOMO \rightarrow LUMO(98) |
| <i>trans</i> - β -carotene | 2.39 | 3.99 | −20.94 | −0.35 | 0.10 | 20.95 | HOMO \rightarrow LUMO(94) |
| zeaxanthin | 2.35 | 4.15 | 21.43 | 2.40 | −0.08 | 21.57 | HOMO \rightarrow LUMO(94) |

^aAs determined with TDDFT at the tuned-LC-BLYP/6-31G(d,p) level of theory.

LUMO). We also note that the zeaxanthin and *trans*- β -carotene show the highest transition dipole moment (μ_{01}) representing highest oscillator strength (f) values since HOMO and LUMO are fully delocalized on the main chain.

SUMMARY AND CONCLUSIONS

In this manuscript we have shown that for systems with short conjugation pathway, the gap-fitting procedure in the LRC functionals provides an improved description of the excited states in comparison to the B3LYP functional. We also highlight that this approach must be used with caution in systems with long conjugation pathway because it is known that DFT-based methods fail to accurately describe the BLA of long polyenic chains.³⁴ However, this approach clearly provides a better description of a set of carotenoid molecules that due to their important role for life^{1,2,43} and its potential as active materials in molecular electronic devices, will be useful in the design and study of similar molecules.

ASSOCIATED CONTENT

Supporting Information

The Supporting Information is available free of charge on the ACS Publications website at DOI: 10.1021/acs.jpca.5b12570.

Tuned range separated parameter (ω) for the ionization potential, electron affinity and gap of the phytofluene, orbital plots for the carotenoids determined by tuned LC-BLYP and ω B97, absorption spectra of the carotenoids computed at the ω B97, vertical transition energies, oscillator strengths, transition dipole moments, and electronic configuration determined at TD- ω B97 level of theory. (PDF)

AUTHOR INFORMATION

Corresponding Author

*E-mail: dasf@unb.br. Phone: +55 (61)3107-0485. Fax: +55 (61)3107-7712.

Notes

The authors declare no competing financial interest.

ACKNOWLEDGMENTS

DASF gratefully acknowledges the financial support from the Brazilian Research Councils: CAPES, CNPq (Grant Nos. 407682/2013-9 and 306968/2013-4) and FAP-DF (Fundação de Apoio a Pesquisa do Distrito Federal).

REFERENCES

- (1) Britton, G.; Liaaen-Jensen, S.; Pfander, H. *Carotenoids: Handbook* 2004, 547.
- (2) Etminan, M.; Takkouche, B.; Caamano-Isorna, F. The Role of Tomato Products and Lycopene in the Prevention of Prostate Cancer:

A Meta-Analysis of Observational Studies. *Cancer Epidemiol Biomarkers Prev* 2004, 13, 340–345.

(3) da Cunha, W. F.; Ribeiro Junior, L. A.; Gargano, R.; e Silva, G. M. Critical Temperature and Products of Intrachain Polaron Recombination in Conjugated Polymers. *Phys. Chem. Chem. Phys.* 2014, 16, 17072–17080.

(4) Ruiz-Anchondo, T.; Flores-Holguin, N.; Glossman-Mitnik, D. Natural Carotenoids as Nanomaterial Precursors for Molecular Photovoltaics: A Computational DFT Study. *Molecules* 2010, 15, 4490–4510.

(5) Hug, H.; Bader, M.; Mair, P.; Glatzel, T. Biophotovoltaics: Natural Pigments in Dye-Sensitized Solar Cells. *Appl. Energy* 2014, 115, 216–225.

(6) Durães, J. A.; Drummond, A. L.; Pimentel, T. A. P. F.; Murta, M. M.; Bicalho, F. S.; Moreira, S. G. C.; Sales, M. J. A. Absorption and Photoluminescence of Buriti Oil/Polystyrene and Buriti Oil/Poly-(Methyl Methacrylate) Blends. *Eur. Polym. J.* 2006, 42, 3324–3332.

(7) Martins, J. B. L.; Durães, J. A.; Sales, M. J. A.; Vilela, A. F. A.; e Silva, G. M.; Gargano, R. Theoretical Investigation of Carotenoid Ultraviolet Spectra. *Int. J. Quantum Chem.* 2009, 109, 739–745.

(8) Schlemmer, D.; Sales, M. J. A.; Resck, I. S. Degradation of Different Polystyrene/Thermoplastic Starch Blends Buried in Soil. *Carbohydr. Polym.* 2009, 75, 58–62.

(9) Lumpi, D.; Horkel, E.; Plasser, F.; Lischka, H.; Frohlich, J. Synthesis, Spectroscopy, and Computational Analysis of Photoluminescent Bis(aminophenyl)-Substituted Thiophene Derivatives. *ChemPhysChem* 2013, 14, 1016–1024.

(10) Coccia, E.; Varsano, D.; Guidoni, L. Ab Initio Geometry and Bright Excitation of Carotenoids: Quantum Monte Carlo and Many Body Green's Function Theory Calculations on Peridinin. *J. Chem. Theory Comput.* 2014, 10, 501–506.

(11) Polli, D.; Antognazza, M. R.; Brida, D.; Lanzani, G.; Cerullo, G.; De Silvestri, S. Broadband Pump-Probe Spectroscopy with sub-10-fs Resolution for Probing Ultrafast Internal Conversion and Coherent Phonons in Carotenoids. *Chem. Phys.* 2008, 350, 45–55.

(12) Ribeiro, L. A.; da Cunha, W. F.; de Oliveria Neto, P. H.; Gargano, R.; e Silva, G. M. Effects of Temperature and Electric Field Induced Phase Transitions on the Dynamics of Polarons and Bipolarons. *New J. Chem.* 2013, 37, 2829–2836.

(13) Lee, C. T.; Yang, W. T.; Parr, R. G. Development of the Colle-Salvetti Correlation-Energy Formula into a Functional of the Electron Density. *Phys. Rev. B: Condens. Matter Mater. Phys.* 1988, 37, 785–789.

(14) Becke, A. D. Density-Functional Exchange-Energy Approximation with Correct Asymptotic Behavior. *Phys. Rev. A: At, Mol., Opt. Phys.* 1988, 38, 3098–3100.

(15) Becke, A. D. Density-Functional Thermochemistry. III. The Role of Exact Exchange. *J. Chem. Phys.* 1993, 98, 5648–5652.

(16) Janzen, D. E.; VanDerveer, D. G.; Mehne, L. F.; da Silva Filho, D. A.; Brédas, J. L.; Grant, G. J. Cyclometallated Pt(II) and Pd(II) Complexes with a Trithiacrown Ligand. *Dalton Transactions* 2008, 1872–1882.

(17) Savin, A. *Recent Developments and Applications of Modern Density Functional Theory*; Elsevier, 1996.

(18) Ikura, H.; Tsuneda, T.; Yanai, T.; Hirao, K. A Long-Range Correction Scheme for Generalized-Gradient-Approximation Exchange Functionals. *J. Chem. Phys.* 2001, 115, 3540.

- (19) Körzdörfer, T.; Sears, J. S.; Sutton, C.; Brédas, J. L. Long-Range Corrected Hybrid Functionals for π -conjugated Systems: Dependence of the Range-Separation Parameter on Conjugation Length. *J. Chem. Phys.* **2011**, *135*, 1–6.
- (20) Pandey, L.; Doiron, C.; Sears, J. S.; Brédas, J. L. Lowest Excited States and Optical Absorption Spectra of Donor-Acceptor Copolymers for Organic Photovoltaics: A New Picture Emerging from Tuned Long-Range Corrected Density Functionals. *Phys. Chem. Chem. Phys.* **2012**, *14*, 14243–14248.
- (21) Dreuw, A.; Weisman, J. L.; Head-Gordon, M. Long-Range Charge-Transfer Excited States in Time-Dependent Density Functional Theory Require Non-Local Exchange. *J. Chem. Phys.* **2003**, *119*, 2943.
- (22) Tawada, Y.; Tsuneda, T.; Yanagisawa, S.; Yanai, T.; Hirao, K. A Long-Range-Corrected Time-Dependent Density Functional Theory. *J. Chem. Phys.* **2004**, *120*, 8425.
- (23) da Silva Filho, D. A.; Friedlein, R.; Coropceanu, V.; Ohrwall, G.; Osikowicz, W.; Suess, C.; Sorensen, S. L.; Svensson, S.; Salaneck, W. R.; Brédas, J. L. Vibronic Coupling in the Ground and Excited States of the Naphthalene Cation. *Chem. Commun.* **2004**, *15*, 1702–1703.
- (24) Kronik, L.; Stein, T.; Refaely-Abramson, S.; Baer, R. Excitation Gaps of Finite-Sized Systems from Optimally Tuned Range-Separated Hybrid Functionals. *J. Chem. Theory Comput.* **2012**, *8*, 1515–1531.
- (25) Kuritz, N.; Stein, T.; Baer, R.; Kronik, L. Charge-Transfer-Like $\pi \rightarrow \pi^*$ Excitations in Time-Dependent Density Functional Theory: A Conundrum and Its Solution. *J. Chem. Theory Comput.* **2011**, *7*, 2408–2415.
- (26) Baer, R.; Livshits, E.; Salzner, U. Tuned Range-Separated Hybrids in Density Functional Theory. *Annu. Rev. Phys. Chem.* **2010**, *61*, 85–109.
- (27) Lima, I. T.; Risko, C.; Aziz, S. G.; da Silva Filho, D. A.; Brédas, J. L. Interplay of Alternative Conjugated Pathways and Steric Interactions on the Electronic and Optical Properties of Donor-Acceptor Conjugated Polymers. *J. Mater. Chem. C* **2014**, *2*, 8873–8879.
- (28) Francl, M. M.; Pietro, W. J.; Hehre, W. J.; Binkley, J. S.; Gordon, M. S.; Defrees, D. J.; Pople, J. A. Self-Consistent Molecular Orbital Methods. XXIII. A Polarization-Type Basis Set for Second-Row Elements. *J. Chem. Phys.* **1982**, *77*, 3654–3665.
- (29) Hariharan, P. C.; Pople, J. A. The Influence of Polarization Functions on Molecular Orbital Hydrogenation Energies. *Theor. Chim. Acta* **1973**, *28*, 213–222.
- (30) Kjelstrup-Hansen, J.; Norton, J. E.; Filho, D. A.; Brédas, J. L.; Rubahn, H. G. Charge Transport in Oligo Phenylene and Phenylene-Thiophene Nanofibers. *Org. Electron.* **2009**, *10*, 1228–1234.
- (31) Chai, J. D.; Head-Gordon, M. Systematic Optimization of Long-Range Corrected Hybrid Density Functionals. *J. Chem. Phys.* **2008**, *128*, 1–15.
- (32) Frisch, M. J.; Trucks, G. W.; Schlegel, H. B.; Scuseria, G. E.; Robb, M. A.; Cheeseman, J. R.; Scalmani, G.; Barone, V.; Mennucci, B.; Petersson, G. A.; et al. *Gaussian 09*, Revision D.01; Gaussian Inc: Wallingford, CT, 2009.
- (33) Stein, T.; Eisenberg, H.; Kronik, L.; Baer, R. Fundamental Gaps in Finite Systems from Eigenvalues of a Generalized Kohn-Sham Method. *Phys. Rev. Lett.* **2010**, *105*, 1–4.
- (34) Körzdörfer, T.; Parrish, R. M.; Sears, J. S.; Sherrill, C. D.; Brédas, J. L. On the Relationship Between Bond-Length Alternation and Many-Electron Self-Interaction Error. *J. Chem. Phys.* **2012**, *137*, 1–8.
- (35) Brédas, J. L.; Adant, C.; Tackx, P.; Persoons, A.; Pierce, B. M. Third-Order Nonlinear Optical Response in Organic Materials: Theoretical and Experimental Aspects. *Chem. Rev.* **1994**, *94*, 243–278.
- (36) Jacquemin, D.; Perpète, E. A.; Scalmani, G.; Frisch, M. J.; Kobayashi, R.; Adamo, C. Assessment of the Efficiency of Long-Range Corrected Functionals for Some Properties of Large Compounds. *J. Chem. Phys.* **2007**, *126*, 144105.
- (37) Peach, M. J. G.; Tellgren, E. I.; Salek, P.; Helgaker, T.; Tozer, D. J. Structural and Electronic Properties of Polyacetylene and Polyynes from Hybrid and Coulomb-Attenuated Density Functionals. *J. Phys. Chem. A* **2007**, *111*, 11930–11935.
- (38) Takaichi, S. Characterization of Carotenes in a Combination of a C18 HPLC Column With Isocratic Elution and Absorption Spectra With a Photodiode-Array Detector. *Photosynth. Res.* **2000**, *65*, 93–99.
- (39) Rodríguez, A. M.; Sastre, S.; Ribot, J.; Palou, A. Beta-Carotene Uptake and Metabolism in Human Lung Bronchial Epithelial Cultured Cells Depending on Delivery Vehicle. *Biochim. Biophys. Acta, Mol. Basis Dis.* **2005**, *1740*, 132–138.
- (40) Craft, N. E.; Soares, J. H., Jr. Relative Solubility, Stability, and Absorptivity of Lutein and Beta-Carotene in Organic Solvents. *J. Agric. Food Chem.* **1992**, *40*, 431–434.
- (41) Macpherson, A. N.; Gillbro, T. Solvent Dependence of the Ultrafast $S_2 \rightarrow S_1$ Internal Conversion Rate of β -Carotene. *J. Phys. Chem. A* **1998**, *102*, 5049–5058.
- (42) Horvin Billsten, H.; Zigmantas, D.; Sundstrom, V.; Polivka, T. Dynamics of Vibrational Relaxation in the S_1 State of Carotenoids Having 11 Conjugated C=C Bonds. *Chem. Phys. Lett.* **2002**, *355*, 465–470.
- (43) Frank, H. A.; Violette, C. A.; Trautman, J. K.; Shreve, A. P.; Owens, T. G.; Albrecht, A. C. Carotenoids in Photosynthesis: Structure and Photochemistry. *Pure Appl. Chem.* **1991**, *63*, 109–114.